Distinct functionality of dishevelled isoforms on Ca^{2+}/calmodulin-dependent protein kinase 2 (CamKII) in *Xenopus* gastrulation

Marc Gentzel[a,*], Carolin Schille[b,*], Verena Rauschenberger[b], and Alexandra Schambony[b]
[a]Max Planck Institute of Molecular Cell Biology and Genetics, 01307 Dresden, Germany; [b]Biology Department, Developmental Biology, Friedrich-Alexander University Erlangen-Nuremberg, 91058 Erlangen, Germany

ABSTRACT **Wnt ligands trigger the activation of a variety of β-catenin–dependent and β-catenin–independent intracellular signaling cascades. Despite the variations in intracellular signaling, Wnt pathways share the effector proteins frizzled, dishevelled, and β-arrestin. It is unclear how the specific activation of individual branches and the integration of multiple signals are achieved. We hypothesized that the composition of dishevelled–β-arrestin protein complexes contributes to signal specificity and identified CamKII as an interaction partner of the dishevelled–β-arrestin protein complex by quantitative functional proteomics. Specifically, we found that CamKII isoforms interact differentially with the three vertebrate dishevelled proteins. Dvl1 is required for the activation of CamKII and PKC in the Wnt/Ca^{2+} pathway. However, CamKII interacts with Dvl2 but not with Dvl1, and Dvl2 is necessary to mediate CamKII function downstream of Dvl1 in convergent extension movements in *Xenopus* gastrulation. Our findings indicate that the different Dvl proteins and the composition of dishevelled–β-arrestin protein complexes contribute to the specific activation of individual branches of Wnt signaling.**

Monitoring Editor
Marianne Bronner
California Institute of Technology

Received: Jun 12, 2014
Revised: Dec 23, 2014
Accepted: Dec 29, 2014

INTRODUCTION

The wingless/integrated-1 protein (Wnt) ligands are glycosylated and palmitoylated paracrine growth factors that regulate patterning, cell migration, and differentiation in embryonic development and adult tissue homeostasis. Deregulated Wnt signaling is often associated with pathological disorders, including cancer and metabolic and neurodegenerative diseases (Cadigan and Nusse, 1997; Logan and Nusse, 2004; Clevers, 2006; Minami *et al.*, 2010). Cellular signaling triggered by Wnt ligands is generally subdivided into the β-catenin–dependent pathway activated by a frizzled and low density lipoprotein receptor–related protein 5/6 (LRP5/6) receptor complex (Brown *et al.*, 1998; Tamai *et al.*, 2000) and multiple β-catenin–independent pathways, which are activated by frizzled and often in combination with a coreceptor of the receptor-tyrosine-kinase family such as Ror2 (Oishi *et al.*, 2003; Nishita *et al.*, 2010), Ryk (Kim *et al.*, 2008), or PTK7 (Lu *et al.*, 2004; Semenov *et al.*, 2007; Verkaar and Zaman, 2010; van Amerongen, 2012).

In the Wnt/β-catenin pathway, the frizzled–LRP5/6 receptor complex recruits intracellular effector proteins, including β-arrestin (Arrb; Bryja *et al.*, 2007), axin, dishevelled (Dvl), glycogen-synthase kinase 3β (GSK3β; Bilic *et al.*, 2007; Kim *et al.*, 2013), and casein kinase 1 (CK1; Davidson *et al.*, 2005) and inhibits the activity of axin and GSK3β in the β-catenin destruction complex (Behrens *et al.*, 1998; Itoh *et al.*, 1998; Farr *et al.*, 2000). As a consequence, β-catenin accumulates in the cytoplasm and translocates into the nucleus, where it acts as a transcriptional coactivator with LEF/TCF transcription factors (McKendry *et al.*, 1997; Kries *et al.*, 2000).

Among the β-catenin–independent signaling cascades, the planar cell polarity (PCP) pathway (reviewed in Wu and Mlodzik, 2009) and the Wnt/Ca^{2+} pathway (reviewed in Kühl *et al.*, 2000b) have been characterized in more detail. In the Wnt/PCP pathway, activation of the receptor complex also induces recruitment of

This article was published online ahead of print in MBoC in Press (http://www.molbiolcell.org/cgi/doi/10.1091/mbc.E14-06-1089) on January 7, 2015.

*These authors contributed equally.

Address correspondence to: Alexandra Schambony (alexandra.schambony@fau.de).

Abbreviations used: CamKII, Ca^{2+}/calmodulin-dependent protein kinase 2; LRP, low density lipoprotein receptor–related protein; Wnt, wingless/integrated-1 protein.

dishevelled (Strutt *et al.*, 1997; Boutros *et al.*, 1998; Wallingford *et al.*, 2000) and β-arrestin (Bryja *et al.*, 2008). However, in this signaling cascade, dishevelled mediates the activation of the Rho-family small GTPases RhoA and Rac1 (Strutt *et al.*, 1997; Habas *et al.*, 2001, 2003) and their downstream effector kinases Rho-associated protein kinase (ROCK; Marlow *et al.*, 2002; Simões *et al.*, 2010) and c-jun N-terminal kinase (JNK; Boutros *et al.*, 1998; Yamanaka *et al.*, 2002; Rosso *et al.*, 2005). The Wnt/Ca^{2+} pathway is characterized by the release of intracellular Ca^{2+} stores (Slusarski *et al.*, 1997b) and subsequent activation of Ca^{2+}-dependent proteins, including protein kinase C (PKC; Sheldahl *et al.*, 1999), Ca^{2+}/calmodulin-dependent protein kinase 2 (CamKII; Kühl *et al.*, 2000a), and the protein phosphatase calcineurin (Saneyoshi *et al.*, 2002). In addition to Wnt ligands, it has been shown that dishevelled is able to activate Ca^{2+} signaling in *Xenopus* embryos (Slusarski *et al.*, 1997a; Sheldahl *et al.*, 1999, 2003; Kühl *et al.*, 2000a).

The different Wnt signaling cascades share a number of proteins, which include Wnt ligands and frizzled receptors, as well as dishevelled, β-arrestin, GSK3β, and CK1. It is becoming more and more evident that Wnt pathways and particularly the variety of β-catenin–independent signaling cascades are often tightly intertwined. However, it is remains unclear how the activation of specific downstream effectors is achieved and how different signal inputs are integrated into a cellular response.

Individual Wnt pathways regulate distinct processes in embryonic development that require their specific, concerted, and tightly controlled activation in time and space. The Wnt/β-catenin pathway is involved in the establishment of the embryonic body axes and embryonic patterning (Funayama *et al.*, 1995; Miller and Moon, 1996; Schneider *et al.*, 1996; Dorsky *et al.*, 1998; Kengaku *et al.*, 1998; Maloof *et al.*, 1999; Kiecker and Niehrs, 2001), as well as in the regulation of cell proliferation and differentiation (Kispert *et al.*, 1998; Tetsu and McCormick, 1999; Dunn *et al.*, 2000; Huelsken *et al.*, 2001; Li *et al.*, 2002; Nakamura *et al.*, 2003). By contrast, the β-catenin–independent Wnt pathways directly influence cytoskeleton organization, cell morphology, cell polarity, and cell motility via the small GTPases, ROCK, PKC, and CamKII and are also essential for the establishment of planar cell polarity and the regulation of cell movements (Moon *et al.*, 1993; Strutt *et al.*, 1997; Heisenberg *et al.*, 2000; Tada and Smith, 2000; Habas *et al.*, 2001; Wallingford *et al.*, 2001; Darken *et al.*, 2002; Bastock *et al.*, 2003; Jenny *et al.*, 2003; Unterseher *et al.*, 2004; Dabdoub and Kelley, 2005; Schambony and Wedlich, 2007; Gao *et al.*, 2011; Ho *et al.*, 2012; Seitz *et al.*, 2014).

In previous work we showed that dishevelled and β-arrestin are required in both β-catenin–dependent and –independent Wnt signaling to relay the signal to downstream effector proteins (Bryja *et al.*, 2007, 2008; Seitz *et al.*, 2014). We hypothesized that the composition of dishevelled/β-arrestin protein complexes varies depending on Wnt signaling activity and that the recruitment of defined interaction partners might contribute to the directing of signaling activity toward specific downstream cascades. To characterize dishevelled/β-arrestin protein complexes and the molecular interactions that contribute to the activation of different Wnt signaling pathways, we carried out interactome studies using quantitative functional proteomics. In particular, we identified CamKIIδ as one protein that exhibits differential interaction with dishevelled/β-arrestin. CamKII is an effector kinase in the Wnt/Ca^{2+} pathway (Kühl *et al.*, 2000a) and was previously reported to antagonize Wnt/β-catenin signaling (Kühl *et al.*, 2001). Therefore we investigated the interactions between the three *Xenopus* members of the Dvl protein family and CamKII and their functional interaction in Wnt/Ca^{2+} signaling in human cells and in *Xenopus* embryos.

RESULTS

CamKII physically interacts with dishevelled 2

We demonstrated recently that β-arrestin 2 (Arrb2), dishevelled 2 (Dvl2), and the β and γ subunits of trimeric G-proteins, respectively Gβ and Gγ (Gβγ), interact physically and functionally in Wnt/Ca^{2+} signaling (Seitz *et al.*, 2014). Along this line, we performed quantitative functional proteomic experiments with Arrb2 as bait protein and identified CamKII as a novel binding partner of the Arrb2-Dvl2-Gβγ complex (Table 1). Quantitative analysis further revealed that coaffinity was substoichiometric relative to the bait protein, but the estimated relative interactor/bait ratio was comparable to the ratio obtained for known Arrb2- or Dvl-interacting proteins such as CK1 (Peters *et al.*, 1999; Sakanaka *et al.*, 1999) and CK2 (Willert *et al.*, 1997).

Consequently we performed the inverse experiment by coimmunopurification of the Arrb2-Dvl2-Gβγ protein complex using Dvl2–green fluorescent protein (GFP) as bait protein. Of interest, we observed an approximate fivefold increased recovery of CamKII (Table 1). These results were in agreement with the previous experiments and indicated a physical interaction of CamKII,

Bait	**Arrb2-Flag**	**Bait**	**Dvl2-GFP**
Coexpressed	Dvl2-GFP	Coexpressed	Arrb2-Flag
	HA-Gβ		HA-Gβ
	HA-Gγ		HA-Gγ
Copurified CamKII: total abundance relative to bait 0.18%		Copurified CamKII: total abundance relative to bait 0.9%	
Peptides identified	**Protein**	**Peptides identified**	**Protein**
AGAYDFPSPEWDTVTPEAK	CamKIIα, β, γ, δ	AGAYDFPSPEWDTVTPEAK	CamKIIα, β, γ, δ
		DLKPENLLLASK	CamKIIα, β, γ, δ
ESTESSNTTIEDEDVK	CamKIIδ	ESTESSNTTIEDEDVK	CamKIIδ
FTDEYQLFEELGK	CamKIIδ	FTDEYQLFEELGK	CamKIIδ

The indicated proteins were expressed transiently in HEK 293T cells, and the Arrb2/Dvl2 protein complexes were isolated by anti-Flag immunoaffinity purification. CamKIIδ was identified in Arrb2-Flag pull downs with three peptides and in Flag-Dvl2 pull downs with 10 peptides. Only peptides with a Mascot Score >20 were considered, and relative quantification to the bait was based on the most intensive three peptides (Vasilj *et al.* 2012). Isoform specificity of peptides was obtained from the proteomicsdb database (www.proteomicsdb.org; Wilhelm *et al.*, 2014).

TABLE 1: Identification of CamKIIδ as a binding partner of Arrb2-Dvl2-Gβγ protein complexes by quantitative functional proteomics.

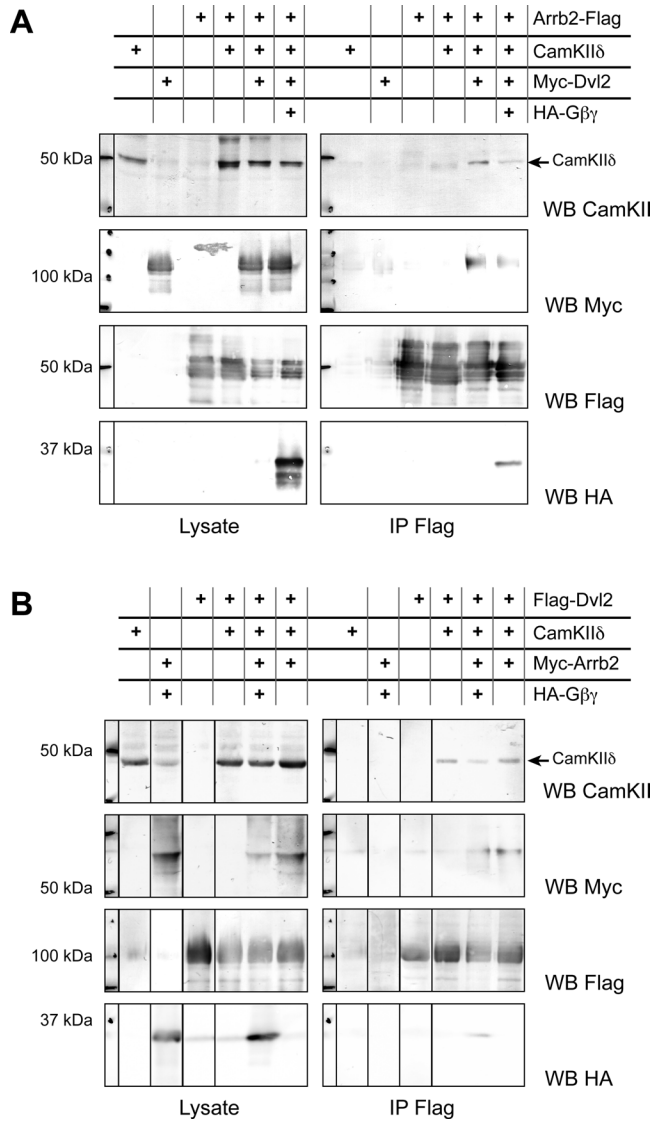

FIGURE 1: CamKIIδ interacts with the Arrb2-Dvl2-Gβγ complex. (A) The interaction was confirmed by coimmunoprecipitation of the respective proteins overexpressed in HEK 293T cells. CamKIIδ coimmunoprecipitated with Flag-Arrb2 only in the presence of Dvl2; in cells coexpressing Gβγ, less Myc-Dvl2 and correspondingly less CamKIIδ was detected in the immunoprecipitate. (B) CamKIIδ was coimmunoprecipitated with Flag-Dvl2 from HEK 293T cells; coexpression of Myc-Arrb2 and Gβγ reduced the overall expression levels of CamKIIδ and the amount coprecipitated with Flag-Dvl2; coexpression of Myc-Arrb2 slightly enhanced the interaction of Flag-Dvl2 with CamKIIδ.

presumably with Dvl2. Two of the identified peptides were not isoform specific; the additional two peptides were unique to CamKIIδ, indicating that CamKIIδ was the predominant isoform bound to the Arrb2-Dvl2-Gβγ protein complex.

We further recapitulated and confirmed the functional proteomic experiments by Western blot analysis. Expression of Arrb2 alone was not sufficient to coprecipitate CamKIIδ, whereas coexpression of Arrb2 and Dvl2 led to efficient enrichment of CamKIIδ in the immunoprecipitate (Figure 1A). Additional coexpression of G-proteins Gβγ reduced the amount of CamKIIδ copurified with Arrb2-Flag, but in addition, the overall expression level of CamKIIδ was decreased (Figure 1A). By contrast, expression of Dvl2 efficiently coenriched CamKIIδ in the respective immunoprecipitations even in the absence of exogenous Arrb2 (Figure 1B), which further supported the assumption of a physical interaction between CamKIIδ and Dvl2. Again, coexpression of Arrb2 enhanced the interaction, whereas coexpression of Arrb2 and Gβγ seemed to decrease the amount of coenriched CamKIIδ (Figure 1B).

Differential interaction between isoforms of Dvl and CamKII

CamKII is an intracellular effector protein of calcium-activated signaling cascades, including the Wnt/Ca^{2+} pathway (Sheldahl *et al.*, 1999, 2003; Kühl *et al.*, 2000a; Seitz *et al.*, 2014). We recently showed that Arrb2 is required for Wnt/Ca^{2+} signaling and that all three vertebrate Dvl isoforms interact with Arrb2 and Gβγ (Seitz *et al.*, 2014). This raised the question of whether CamKII binds preferentially to a particular Dvl. We overexpressed and immunoprecipitated Myc-tagged Dvl1, Dvl2, or Dvl3 in HEK293T cells. Surprisingly, endogenous CamKII coprecipitated selectively with Dvl2 but not with Dvl1 or Dvl3 (Figure 2A). Stimulation of the cells with Wnt-5a–conditioned medium enhanced the interaction of CamKII with Dvl2, and we were also able to detect a very weak interaction of CamKII with Dvl3 in these stimulated cells (Figure 2A). These results indicated that CamKII preferentially interacted with Dvl2. We confirmed this observation in coimmunoprecipitations of Dvl1, Dvl2, and Dvl3 from cells that additionally overexpressed CamKIIδ and CamKIIγ (Supplemental Figure S1). Moreover, this experiment also revealed that CamKIIγ did not interact with any Dvl isoform. This observation prompted us to further investigate the interactions between CamKII and Dvl isoforms.

In coimmunoprecipitation of Dvl1, Dvl2, or Dvl3 with CamKIIα, CamKIIβ, CamKIIγ, and CamKIIδ, we confirmed that Dvl2 strongly interacted with CamKIIδ and additionally with CamKIIβ and CamKIIα (Figure 2B). By contrast, Dvl1 did not interact with any of the CamKII isoforms (Figure 2C). Dvl3 interacted moderately with CamKIIα and CamKIIδ and weakly with CamKIIβ (Figure 2D), but the binding of CamKII isoforms to Dvl3 was overall weaker than the interaction with Dvl2. This is consistent with the detection of an interaction between endogenous CamKII with Dvl3 only after Wnt-5a stimulation and at a much lower level than in Dvl2 immunoprecipitates (Figure 2A).

Dishevelled 1 but not dishevelled 2 activates Wnt/$Ca^{2±}$ signaling in vivo

In early *Xenopus* embryos, CamKII contributes to the establishment of the dorsoventral body axis (Kühl *et al.*, 2000a). During gastrulation, CamKII regulates the separation of mesoderm and ectoderm and is required for convergent extension (CE) movements of the dorsal mesoderm (Winklbauer *et al.*, 2001; Seitz *et al.*, 2014). Therefore we wondered whether in addition to differential physical interaction, Dvl1, Dvl2, and Dvl3 also displayed differential ability to activate or modulate Wnt/Ca^{2+} signaling in *Xenopus* gastrulation.

First, we immunoprecipitated endogenous CamKII from gastrula-stage *Xenopus* embryos overexpressing Myc-tagged Dvl1, Dvl2, or Dvl3. We noted that endogenous CamKII selectively coprecipitated Dvl2 but not Dvl1 or Dvl3 (Figure 3A). These results were consistent with the aforementioned findings showing the strongest interaction between the CamKIIα, β, and δ isoforms and Dvl2 (Figure 2). The interaction between CamKII and Dvl2 was confirmed by endogenous coimmunoprecipitation experiments in *Xenopus* embryos (Figure 3B) and also in human HEK293T cells (Figure 3C). In both experiments, CamKII only coprecipitated when Dvl2 was captured with an anti-Dvl2 antibody but not in the control samples using an unrelated control antibody.

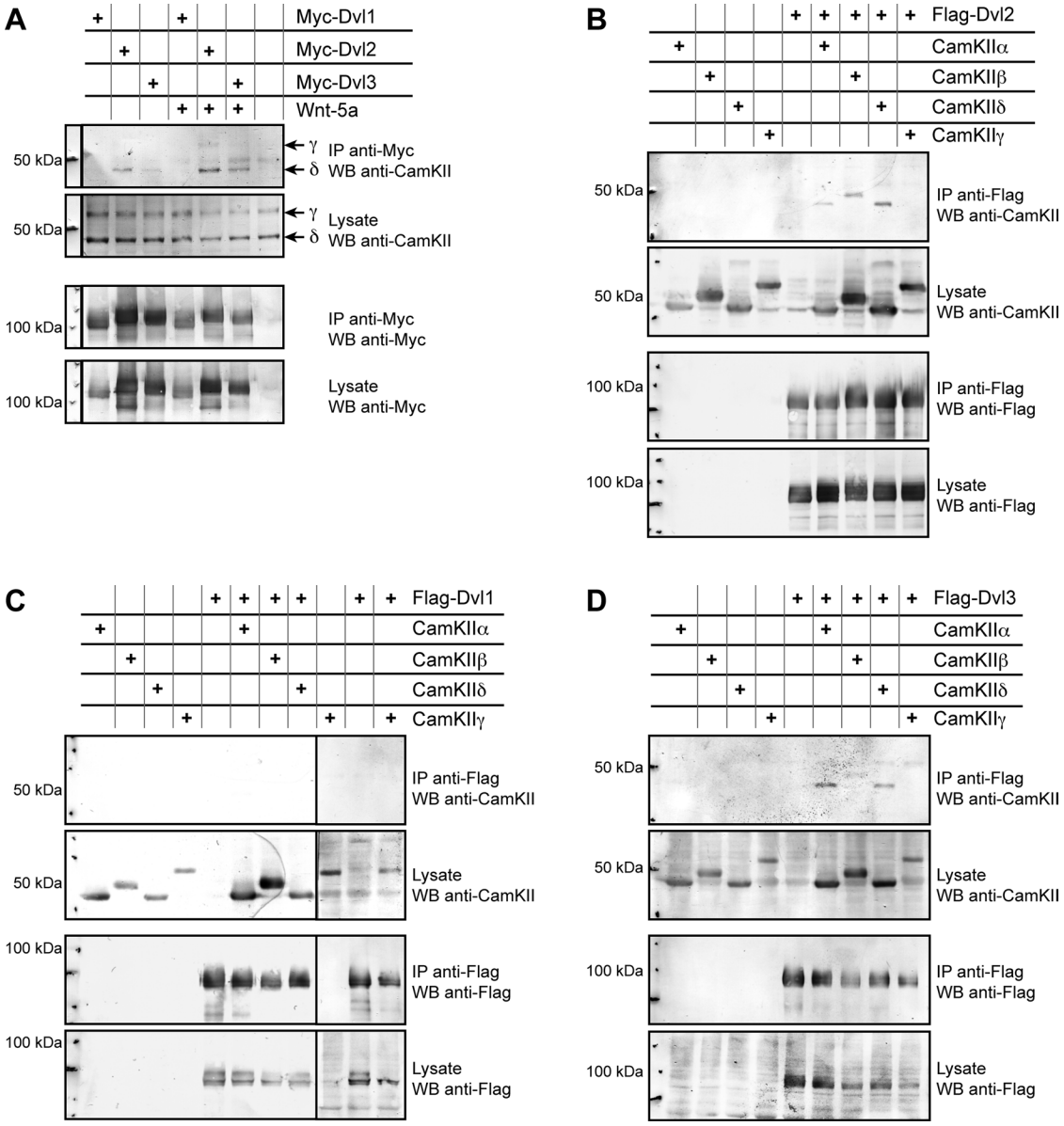

FIGURE 2: Differential interaction between CamKII and Dvl isoforms. (A) Overexpressed Myc-Dvl1, Myc-Dvl2, and Myc-Dvl3 were immunoprecipitated from HEK293T cells and analyzed for coprecipitation of endogenous CamKII. No binding of CamKII to Dvl1 was detectable. CamKII interacted with Dvl2 and very weakly with Dvl3 in unstimulated cells; both interactions were increased upon stimulation with Wnt-5a–conditioned medium for 30 min. To define further the specificity of interaction between CamKII and Dvl isoforms, CamKIIα, CamKIIβ, CamKIIδ, and CamKIIγ were coexpressed with Flag-Dvl2 (B), Flag-Dvl1 (C), or Flag-Dvl3 (D) in HEK 293T cells. The Flag-tagged Dvl isoforms were immunoprecipitated using immobilized anti-Flag antibodies. (B) Flag-Dvl2 bound and coprecipitated CamKIIα, CamKIIβ, and CamKIIδ but not CamKIIγ. (C) Neither CamKIIα nor β, δ, or γ coprecipitated with Flag-Dvl1. (D) Flag- Dvl3 interacted with CamKIIα and CamKIIδ, and weak bands of CamKIIβ and γ were also observed in Dvl3 immunoprecipitates.

Next we investigated the influence of Dvl1, Dvl2, and Dvl3 on CamKII activation in *Xenopus* embryos by immunoblotting against active CamKII autophosphorylated at threonine 286 (pCamKII). Of interest and unexpectedly, we found that overexpression of Dvl1 increased the level of pCamKII, whereas Dvl2 had no effect on CamKII phosphorylation and activation. By contrast, Dvl3 overexpression resulted in a decrease of pCamKII (Figure 4A). Overexpression of Dvl1 in HEK293T cells also increased pCamKII levels (Supplemental Figure S2), which was consistent with our findings in *Xenopus* embryos. These results suggested selective roles for the individual Dvl proteins in signaling to CamKII, which was confirmed by the corresponding single-morpholino knockdown experiments. In Dvl1-morphant embryos, pCamKII levels were decreased and Dvl2 knockdown did not influence pCamKII levels, and in Dvl3 morphants, we detected a marked increase of pCamKII (Figure 4B). In addition, CamKII kinase activity was determined in a mass spectrometry–based kinase activity assay. Consistent with the foregoing results, we also observed an increase in CamKII activity in Dvl1-overexpressing embryos and a corresponding decrease in Dvl1 morphants (Figure 4C). Dvl2 overexpression or knockdown again had no effect, and Dvl3 overexpression led to a decrease and Dvl3 morpholino (MO) injection to an increase in CamKII activity

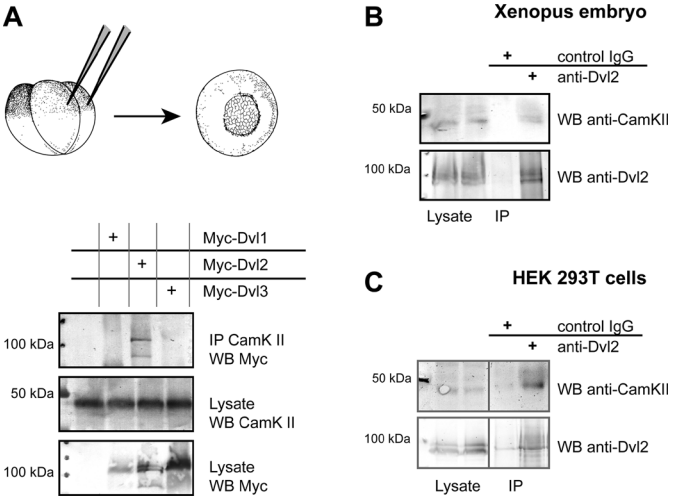

FIGURE 3: Endogenous CamKII interacts with Dvl2 in *Xenopus* embryos. (A) *Xenopus* embryos were injected as illustrated in the two dorsal blastomeres at the four-cell stage with RNA encoding Myc-Dvl1, Myc-Dvl2, or Myc-Dvl3. At early-gastrula stage (NF stage 10.5), endogenous CamKII was captured by immunoaffinity and the immunoprecipitates probed for the presence of the Myc-tagged Dvl isoforms (A). Endogenous CamKII coprecipitated with endogenous Dvl2 from *Xenopus* embryos (B) and from HEK 293T cells (C), confirming the physical interaction.

(Figure 4C). These results were in agreement with CamKII autophosphorylation at T286 (Figure 4, A and B) and confirmed that *Xenopus* Dvl1, Dvl2, and Dvl3 differentially regulate CamKII activation in vivo.

Next we asked whether the observed selective activation of CamKII by Dvl1 was also true for the activation of PKC and thus might indicate differential activity of Dvl isoforms in Wnt/Ca^{2+} signaling in general. PKCα is a Ca^{2+}- and diacylglycerol (DAG)-dependent PKC isoform that translocates to the plasma membrane upon activation and DAG binding. Membrane translocation of PKCα is a commonly used readout for the activation of Wnt/Ca^{2+}-mediated signaling (Sheldahl *et al.*, 1999). PKCα translocation can be induced in *Xenopus* animal cap tissue by overexpression of *Xenopus* Fzd7 (Winklbauer *et al.*, 2001; Seitz *et al.*, 2014). Here we also overexpressed Fzd7 in *Xenopus* embryos to stimulate PKCα-GFP recruitment to the plasma membrane in animal cap tissue (Figure 5, A and B). Coinjection of Dvl1 MO–reduced Fzd7 induced PKCα-GFP translocation to the cell membrane (Figure 5C), whereas coinjection of either Dvl2 MO or Dvl3 MO (Figure 5, D and E) had no effect on PKCα translocation. In the inverse experiment, we coinjected *pkcα-gfp* RNA with subeffective doses of *fzd7* RNA (Figure 5F) and *myc-dvl1*, *myc-dvl2*, or *myc-dvl3* RNA. Consistently, only coexpression of myc-Dvl1 (Figure 5G), and that of neither myc-Dvl2 (Figure 5H) nor myc-Dvl3 (Figure 5I), promoted membrane translocation of PKCα-GFP.

These results indicated that PKC and CamKII are activated in a Dvl1-dependent manner. However, CamKII only selectively interacted with Dvl2, which, astonishingly, had no detectable influence on CamKII phosphorylation or PKC translocation in *Xenopus*.

For further functional analysis, we examined the expression of CamKII during embryogenesis. The antibody used for detection of endogenous *Xenopus* CamKII was not isoform specific, and therefore we analyzed the presence of transcripts encoding the four CamKII isoforms in different developmental stages of *Xenopus* embryos. Of interest, *camkIIδ* transcripts were the most abundant from early cleavage stages until organogenesis (Supplemental Figure S3). *camkIIα* RNA was first detectable in neurula stages (stage 17) and was strongly up-regulated in organogenesis stages (stages 24 and 28). Similarly, *camkIIβ* transcripts were detected only in stage 24 and 28 embryos. Maternal *camkIIγ* transcripts were present in eight-cell-stage and blastula-stage embryos; levels dropped below detection limit during gastrulation and increased again from stage 20 onward (Supplemental Figure S3). These results showed that *camkIIδ* is the most abundant *camkII* transcript in early embryos and the only isoform transcribed throughout gastrulation. Consequently we used CamKIIδ to study further the functional interaction with the three Dvl proteins in *Xenopus* gastrulation.

Noncanonical Wnt pathways, including the Wnt/Ca^{2+} pathway, are required for CE movements in *Xenopus* (Moon *et al.*, 1993; Tada and Smith, 2000; Wallingford *et al.*, 2001), and therefore we investigated the role and potential functional redundancy of Dvl1, Dvl2, and Dvl3 in CE movements.

In Keller open-face explants from Dvl1-morphant embryos, we observed CE defects manifesting predominantly as inhibition of explant elongation (Figure 6A). The Dvl1-morphant phenotype in Keller explants was rescued by overexpression of Dvl1, PKC, or CamKIIδ (Figure 6A). These rescues were consistent with an activating function of Dvl1 in the Wnt/Ca^{2+} pathway and activation of PKCα and CamKII, as shown in Figures 4 and 5. Knockdown of Dvl2 induced less severe elongation defects than Dvl1 MO, but a high percentage of Dvl2-depleted explants showed pronounced constriction defects (Figure 6B and our previous report, Bryja *et al.* 2008). The CE phenotype in Dvl2 morphants was rescued by coinjection of a morpholino-insensitive *myc-dvl2* RNA (Figure 6B). In contrast to Dvl1-depleted explants, overexpression of PKCα was not able to rescue elongation or constriction in explants from Dvl2-morphant embryos, whereas overexpression of CamKIIδ in these explants resulted in an even stronger inhibition of CE movements (Figure 6B). Explants from Dvl3-morphant embryos showed a similar phenotype to Dvl2-depleted explants, namely moderate elongation but significant constriction defects (Figure 6C). The phenotype was also rescued by coinjection of morpholino-insensitive *myc-dvl3* RNA, which confirmed the specificity of the knockdown phenotype. Overexpression of PKCα in Dvl3-morphant embryos resulted in a mild but statistically not significant improvement of CE movements, and overexpression of CamKIIδ had no effect in these explants. In contrast and consistent with the observed enhanced CamKII autophosphorylation in Dvl3-morphant embryos, the CE phenotype in Dvl3-depleted explants was rescued by overexpression of dnCamKIIδ (Figure 6C).

Because Dvl1 activated CamKII whereas Dvl2 physically interacted and appeared to be functionally related to CamKII in *Xenopus* CE movements, we also investigated a potential functional redundancy between Dvl1 and Dvl2 with respect to Wnt/Ca^{2+} signaling. First we tested whether Dvl2 was able to rescue CE movements in Dvl1-morphant explants and vice versa. We observed that Dvl2 indeed rescued the Dvl1-knockdown phenotype in Keller explants. However, in the inverse experiment, Dvl1 was not sufficient to rescue Dvl2 depletion (Figure 6D). Simultaneous knockdown of both Dvl1 and Dvl2, not unexpectedly, resulted in a much more severe inhibition of explant elongation (Figure 6D). Of interest, in Dvl1/Dvl2 double-morphant embryos, coexpression of CamKIIδ restored elongation but not constriction of the explants (Figure 6D), a phenotype highly reminiscent of the single Dvl2-knockdown phenotype

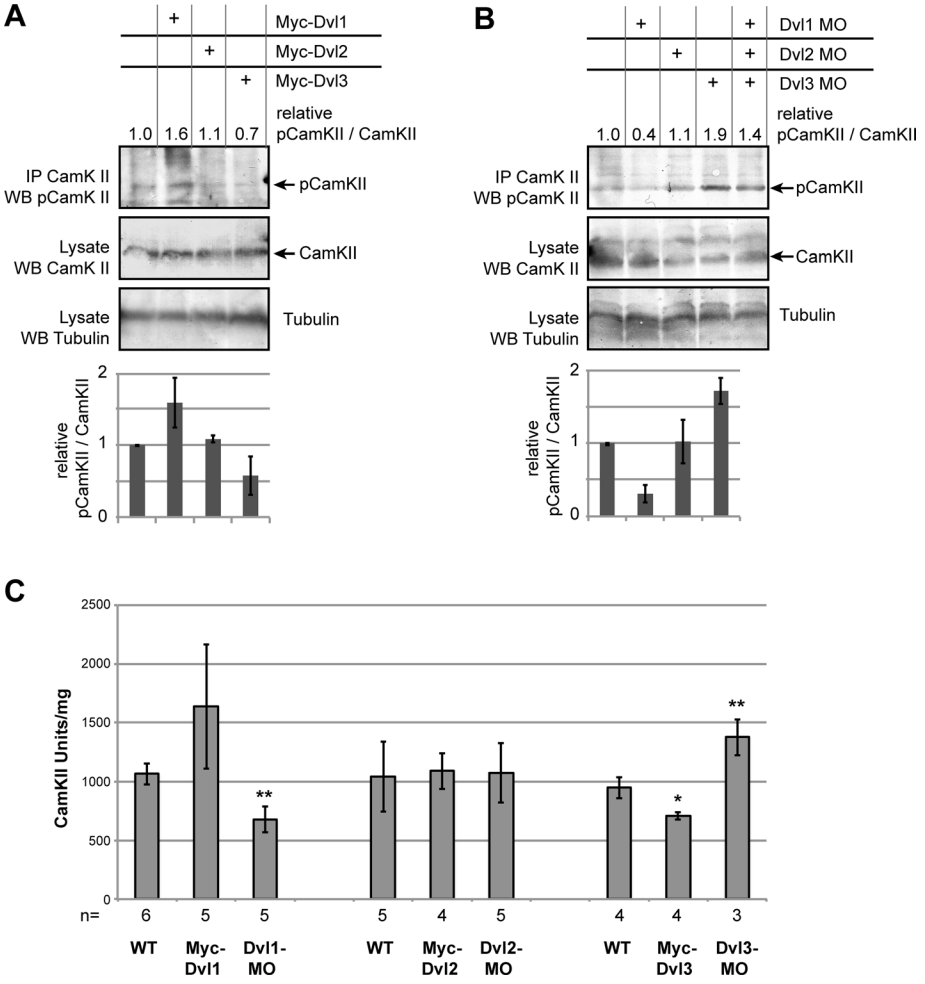

FIGURE 4: Dvl1 activates CamKII in *Xenopus* embryos. (A) Immunoblotting for active CamKII-pT286 showed that Myc-Dvl1, but not Myc-Dvl2, enhanced CamKII phosphorylation, whereas Myc-Dvl3 reduced pCamKII levels in the embryos. (B) Knockdown of individual Dvl isoforms using specific antisense morpholino oligonucleotides yielded the inverse result. Dvl1 morphants showed reduced and Dvl3 morphants showed increased pCamKII levels, whereas Dvl2 knockdown did not affect pCamKII. In triple Dvl-morphant embryos, increased pCamKII levels were again observed. Ratios of pCamKII/CamKII in A and B were determined densitometrically relative to uninjected controls. Values noted above the respective lanes represent measurements of the blots shown; bar graphs below show the average ± SD from three independent experiments. (C) *Xenopus* embryos were injected as indicated, and CamKII kinase activity was measured. The graph represents the average activity from at least three independent experiments (average ± SEM); injections and number of experiments (*n*) are given below the graph. Asterisks indicate statistically significant deviation of means from corresponding wild-type levels (*$p > 0.1$, **$p > 0.05$, Wilcoxon rank-sum test).

(Figure 6D). Taken together, these results indicated that Dvl1 was not sufficient to functionally replace Dvl2, but Dvl2 could compensate Dvl1 loss of function. Moreover it appears that the ability of CamKIIδ to rescue the Dvl1 MO phenotype depended on the presence of Dvl2.

DISCUSSION

Gastrulation in *Xenopus*, as in all vertebrate embryos, is the first morphogenetic process in embryonic development. The three germ layers are specified and positioned relative to each other predominantly by internalization and reorganization of the mesoderm in tightly controlled and coordinated mass cell movements in which β-catenin–independent Wnt pathways play crucial roles (Moon *et al.*, 1993; Tada and Smith, 2000; Wallingford *et al.*, 2001). After specification of the germ layers and vegetal rotation, the mesoderm involutes, beginning at the dorsal blastopore lip (Keller, 2005). The internalized mesoderm is kept separated from the overlying ectoderm, a process mediated by frizzled signaling to PKC (Winklbauer *et al.*, 2001), that is, Wnt/Ca^{2+} signaling. After involution, polarization and mediolateral intercalation behavior is initiated in the dorsal mesoderm, which results in CE, the elongation and mediolateral narrowing of the entire tissue. Cell polarity during CE movements is conferred and maintained by the Wnt/PCP pathway (Goto and Keller, 2002; Wallingford *et al.*, 2002; Unterseher *et al.*, 2004; Jenny and Mlodzik, 2006). In addition, Wnt/Ca^{2+} signaling is also required for CE movements in *Xenopus* (Choi and Han, 2002; Penzo-Mendèz *et al.*, 2003; Seitz *et al.*, 2014). Both signaling pathways play an important role in maintenance and remodeling of cell shape and cell polarity and in the regulation of cell movements. Dissecting the interplay of these signaling events in CE movements is challenging because both β-catenin–independent Wnt pathways are activated by dishevelled and β-arrestin (Sheldahl *et al.*, 2003; Wang *et al.*, 2006; Bryja *et al.*, 2008; Seitz *et al.*, 2014), and we proposed that Dvl-Arrb2 protein complexes act as signaling hubs (Seitz *et al.*, 2014). Moreover, it has been suggested that Wnt signaling should be viewed as an interconnected network rather than as individual signaling cascades (Kestler and Kühl, 2008).

With the identification and characterization of an interaction between CamKII, Dvl2, and β-arrestin, we have demonstrated specific physical interactions within this signaling network. By contrast, dishevelled 1 is required for the activation of PKC and CamKII and functionally links the Wnt/Ca^{2+} pathway to other Dvl- and β-arrestin–dependent Wnt pathways. Arrb2 interacts with all three vertebrate Dvl proteins (Seitz *et al.*, 2014), and both Arrb2 and dishevelled are essential in β-catenin–dependent and –independent Wnt pathways (Bryja *et al.*, 2007, 2008; Seitz *et al.*, 2014). Therefore it could be hypothesized that Arrb2 and Dvl form central protein complexes in Wnt signaling that are modulated in a context-dependent manner, interact with additional proteins as demonstrated here for CamKII, and thereby trigger different cellular responses. Moreover, we observed differential interaction of Dvl1, Dvl2, and Dvl3 with the four CamKII isoforms, which implies that the expression of specific isoforms contributes to the degree of interaction and modulation between these proteins and between different branches of Wnt signaling.

In addition to the physical interaction, we have shown a functional interaction between CamKIIδ and all three Dvl proteins, in particular with Dvl1 and Dvl2, in *Xenopus* gastrulation. Of interest, in gastrula-stage embryos, we detected only transcripts encoding

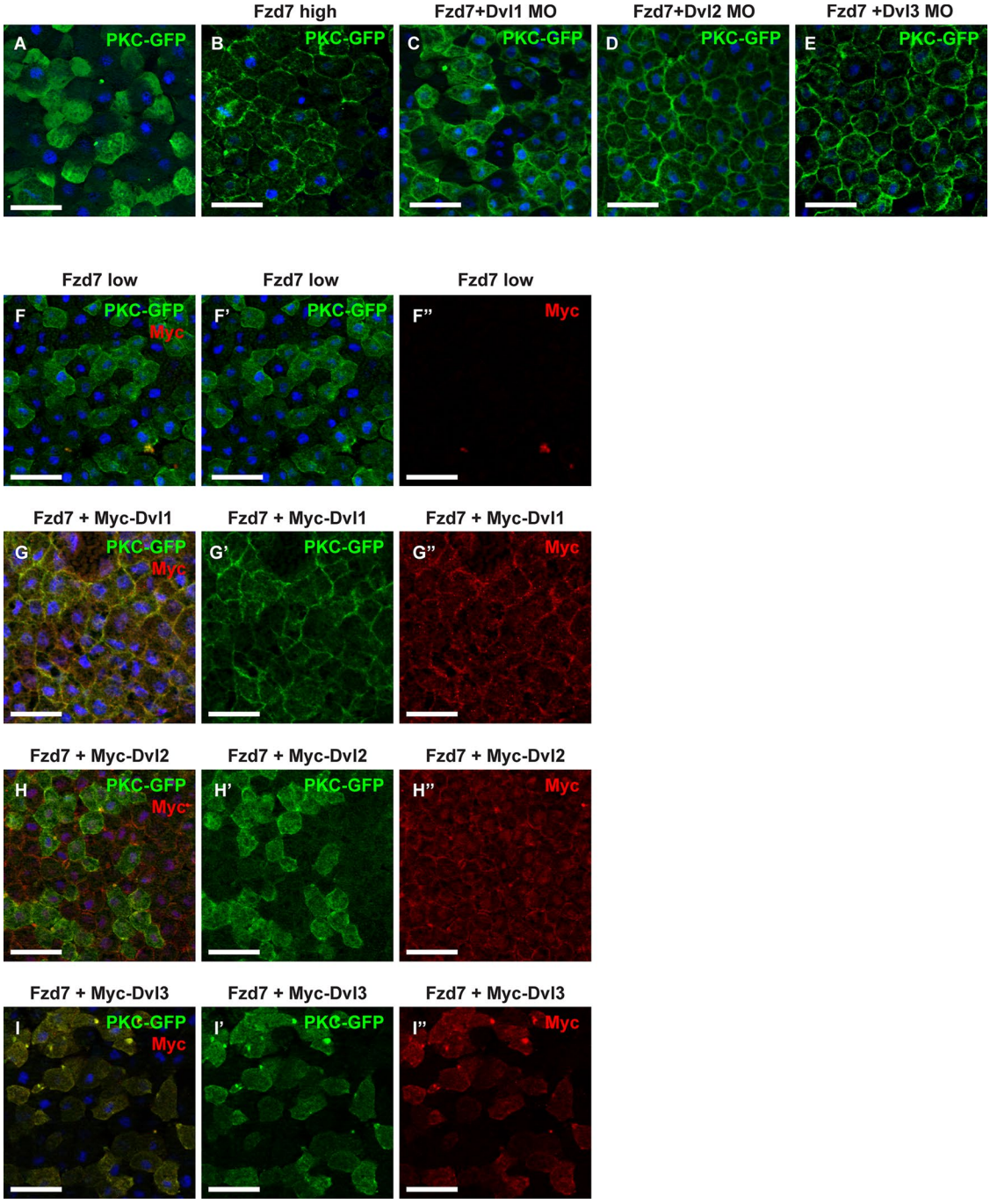

FIGURE 5: Dvl1 is required for activation and membrane translocation of PKC in *Xenopus* embryos. *Xenopus* embryos were injected with 500 pg of *pkcα-gfp* RNA and coinjected as indicated above the images. Animal caps were prepared at stage 10 and immunostained as indicated. Nuclei were stained with Hoechst 33258 (blue). Images show representative results of at least three independent experiments with a minimum of six Animal Caps per experiment. Scale bars, 50 μm. (A) PKCα-GFP predominantly localized to the cytoplasm in *Xenopus* animal caps. (B) Coinjection of 1 ng of *fz7* RNA induced translocation of PKCα-GFP to the plasma membrane, indicating activation of PKC. (C) Overexpression of Fz7 was less effective in inducing PKCα-GFP translocation in Dvl1-morphant embryos. Knockdown of Dvl2 (D) or Dvl3 (E) did not impair Fz7-induced PKC-GFP translocation. Injection of subeffective amounts of *fz7* RNA (300 ng) did not alter PKCα-GFP localization (F, F′) compared with animal cap cells expressing only PKCα-GFP (A). Coinjection of 200 pg of *myc-dvl1* RNA induced robust membrane translocation of PKCα-GFP (G, G′). The tissue was coimmunostained against the Myc epitope, showing that Myc-Dvl1 predominantly localized to the plasma membrane and colocalized with PKCα-GFP (G″). Coinjection of 200 pg of *myc-dvl2* RNA was not sufficient to induce translocation of PKCα-GFP to the plasma membrane (H, H′). Myc-Dvl2 was detected in the cytoplasm and at the plasma membrane (H″). Coinjection of 200 pg of *myc-dvl3* RNA also failed to induce membrane translocation of PKCα-GFP (I, I′). Myc-Dvl3 predominantly localized in the cytoplasm and partially formed large aggregates, which were also positive for PKCα-GFP (I″ and I).

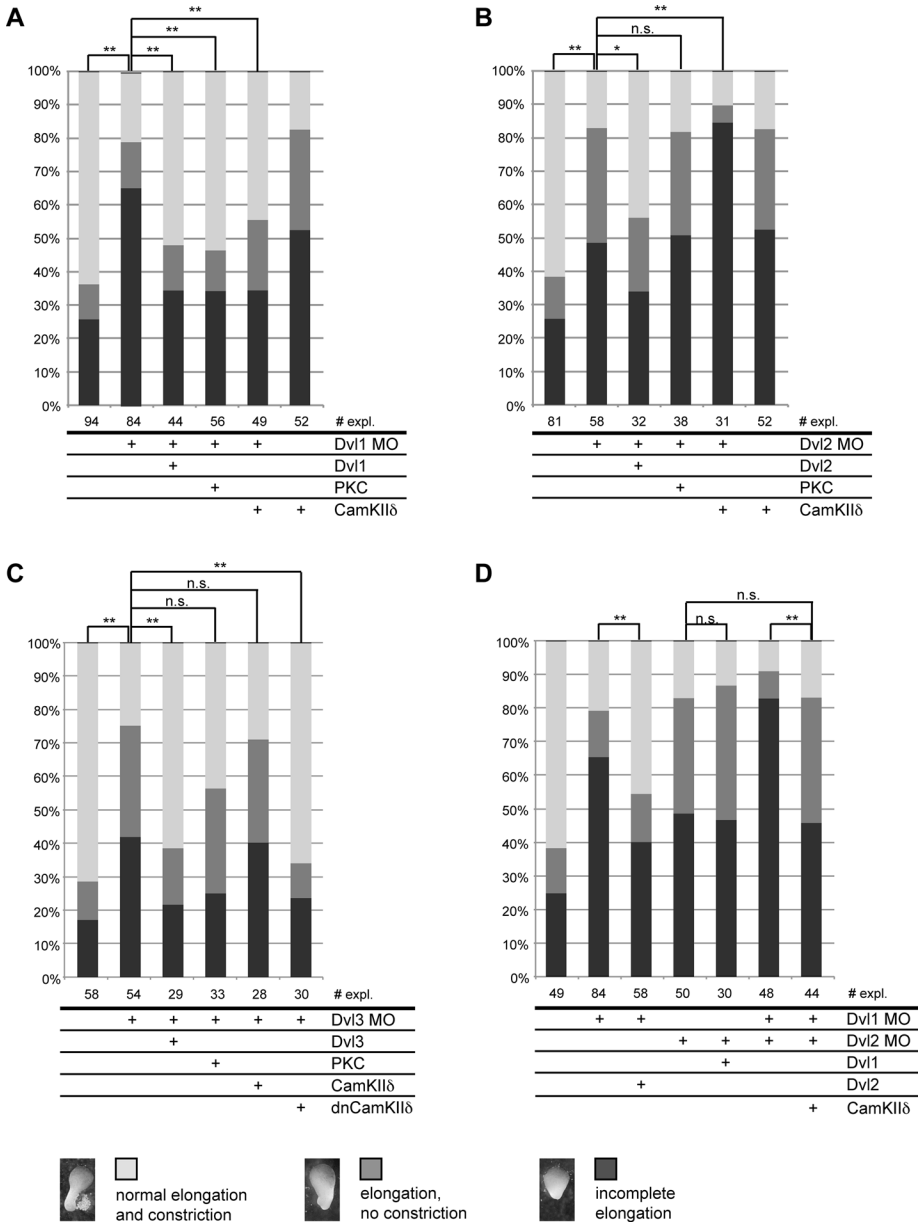

FIGURE 6: CamKIIδ acts downstream of Dvl1 in *Xenopus* convergent extension movements. *Xenopus* embryos were injected at the four-cell stage in the marginal zone of both dorsal blastomeres as indicated. CE movements in the dorsal mesoderm were monitored by elongation and constriction of Keller open-face explants. The average percentage of explants showing full elongation and constriction (light gray), elongation but impaired constriction (medium gray), or incomplete elongation (dark gray) from at least three independent experiments is shown. Asterisks indicate statistically significant deviations (**$p > 0.99$, *$p > 0.95$, χ^2 test). (A) Dvl1 knockdown predominantly inhibited explant elongation. The Dvl1-knockdown phenotype was rescued by overexpression of Dvl1, PKCα, or CamKIIδ; overexpression of CamKIIδ induced moderate elongation and constriction defects. (B) Dvl2 knockdown resulted in a weaker inhibition of elongation but a significant increase in constriction defects. The Dvl2-knockdown phenotype was not rescued by PKCα or CamKIIδ but was rescued by coinjection of a morpholino-insensitive *myc-dvl2* RNA. (C) The Dvl3 knockdown phenotype was similar to the phenotype in Dvl2-depleted explants. Dvl3 MO knockdown was rescued by Dvl3 and partially but statistically not significantly by PKC. CamKIIδ was not able to rescue Dvl3 depletion, but coinjection of an RNA encoding dnCamKIIδ rescued CE movements. (D) Dvl2 overexpression rescued the Dvl1-morphant phenotype, but not vice versa. Explants from Dvl1/Dvl2 double-morphant embryos showed a more severe phenotype than the single knockdowns. Overexpression of CamKIIδ significantly rescued explant elongation but not constriction, thus yielding an explant phenotype highly similar to explants from Dvl2 morphants.

CamKIIδ. CamKIIα and CamKIIβ were expressed only from neurula stages onward, which is consistent with a predominantly neural expression of these CamKII isoforms in rats (Erondu and Kennedy, 1985; Tobimatsu and Fujisawa, 1989). CamKIIδ and CamKIIγ are expressed ubiquitously in rat (Tobimatsu and Fujisawa, 1989); however, in *Xenopus* embryos, CamKIIγ was down-regulated during gastrulation. Consistently, we observed only one band corresponding to the predicted molecular weight of *Xenopus* CamKIIδ protein in lysates from gastrula-stage embryos. In coimmunoprecipitation, we detected interaction of CamKII from *Xenopus* embryos only with Dvl2, which correlated well with the strongest interaction between these two proteins in coimmunoprecipitation experiments with human cells. This strong physical interaction was also detected in and confirmed by coimmunoprecipitation of the endogenous proteins in HEK293T cells and in *Xenopus* embryos.

Despite this physical interaction, Dvl2 did not alter the levels of active autophosphorylated CamKII or CamKII kinase activity in these embryos. By contrast, Dvl1 was required upstream of PKC and CamKII and was sufficient to induce PKC translocation and increase CamKII autophosphorylation and kinase activity in *Xenopus* embryos. The up-regulation of *Xenopus* Dvl1 gene expression at gastrula stages shown by Tadjuidje *et al.* (2011) coincides with the Dvl1-mediated CamKIIδ activation during gastrulation demonstrated here. Of interest, this functional relationship between Dvl1 and CamKII has also been reported in the formation of excitatory synapses in rat spinal neurons (Ciani *et al.*, 2011), indicating that Dvl1 might preferentially signal to the Wnt/Ca^{2+} pathway.

On the other hand, Dvl3 endogenously inhibited CamKII activity, which clearly demonstrated a distinct molecular function of Dvl3 as compared with Dvl1 and Dvl2 in *Xenopus* gastrulation.

Moreover, our findings indicate that regulation of CamKII signaling activity and physical interaction with CamKII are mediated by different Dvl proteins, thus uncoupling these two events. This does not exclude overlapping functions in CE movements or other developmental processes in general, as reported for Dvl2 and Dvl3 in CE movements (Tadjuidje *et al.*, 2011) and for Dvl1 and Dvl2 in neural crest migration (Gray *et al.*, 2009), since these morphogenetic processes are regulated by multiple interacting Wnt pathways. Consistent with the latter report, we also observed that Dvl2 was sufficient to rescue the CE

phenotype in Dvl1-depleted explants. However, Dvl1 did not rescue the Dvl2-morphant phenotype, and CamKIIδ only partially rescued the double knockdown of Dvl1 and Dvl2. Of interest, these explants displayed a phenotype that is highly reminiscent of the single Dvl2 knockdown, suggesting that CamKIIδ acted downstream of Dvl1 but depended on Dvl2 in CE movements.

The molecular mechanism by which a protein complex of Arrb2-Dvl2 and CamKIIδ regulates CE movements remains elusive. CamKII has been shown to act in microtubule reorganization in cortical axons (Li *et al.*, 2014) and regulate the length and frequency of actin-containing filopodia in migrating cancer cells (Wang *et al.*, 2010). Dishevelled likewise modulates both microtubule stability and actin reorganization (Krylova *et al.*, 2000; Ciani and Salinas, 2007; Habas *et al.*, 2001, 2003). Microtubules are required in the initiation of CE movements in *Xenopus* but are dispensable in later phases, when cell migration depends on the actin cytoskeleton (Lane and Keller, 1997). Therefore it is conceivable that CamKIIδ and Dvl2 or, more generally, the Wnt/Ca^{2+} and Wnt/PCP pathways act in concert to control cell shape, cell polarity, and cell migration during CE movements.

MATERIALS AND METHODS

Plasmids and morpholinos

The following plasmids and morpholinos have been described previously: pcDNA-FLAG-*arrb2* (Bryja *et al.*, 2007), pCS2+ *fzd7* (Unterseher *et al.*, 2004), Dvl2 MO (Bryja *et al.*, 2008), and Dvl1 MO and Dvl3 MO (Gray *et al.*, 2009).

The expression plasmid pCS2+ *pkcα-gfp* was generously provided by Michael Kühl (University of Ulm, Ulm, Germany); pcDNA *HA-gβ1* (*HA-gnb1*) and pcDNA *HA-gγ2* (*HA-gng2*) were provided by G. Schulte (Karolinska Institute, Stockholm, Sweden); and expression plasmids encoding human CamKIIα, CamKIIβ, CamKIIγ, and CamKIIδ were a kind gift from Gary Davidson (Karlsruhe Institute of Technology, Karlsruhe, Germany). The open reading frames encoding *Xenopus laevis* CamKIIδ, Dvl1, Dvl2, and Dvl3 were amplified by PCR and cloned into pCS2+ Myc (R. Rupp, Ludwig Maximilian University, Munich, Germany) and pCS2+ Flag; point mutations were introduced in Flag-CamKIIδ by site-directed mutagenesis to generate dominant-negative CamKIIδ K42M and constitutively active CamKIIδ T286D.

Antibodies

Rabbit anti-GFP and rabbit anti-HA were obtained from Abcam (Cambridge, UK), rabbit anti-Myc, rabbit anti-Flag, rabbit anti-pCamKII (pT286), and rabbit anti-GFP from Cell Signaling Technology (Beverly MA), and rabbit anti-Dvl2 from Proteintech (Chicago, IL), and mouse anti-CamKII was purchased from BD Biosciences (Heidelberg, Germany). The anti-Tubulin β hybridoma developed by Michael Klymkowski and the anti-Myc hybridoma clone 9E10 developed by J. Michael Bishop were obtained from the Developmental Studies Hybridoma Bank, created by the National Institute of Child Health and Human Development of the National Institutes of Health and maintained at The University of Iowa, Department of Biology, Iowa City, IA. Secondary antibodies used were anti-mouse alkaline phosphatase and anti-rabbit alkaline phosphatase (Cell Signaling Technology), anti-mouse Cy3 (Jackson ImmunoResearch, West Grove PA), and anti-rabbit Alexa 488 and anti-mouse Alexa 647 (Life Technologies, Carlsbad, CA).

X. laevis embryos

X. laevis embryos were generated and cultured according to general protocols and staged according to the normal table of Nieuwkoop and Faber (1975). All procedures were performed according to the German animal use and care law (Tierschutzgesetz) and approved by the German state administration Bavaria (Regierung von Mittelfranken).

Injection and analysis of *X. laevis* embryos and tissue explants

RNA for microinjection was prepared from the respective plasmids using the mMessage mMachine Kit (Ambion, Austin, TX). If not stated otherwise, injection amounts were 500 pg of *pkcα-gfp*, 50 pg of *myc-dvl1*, *myc-dvl2*, and *myc-dvl3*, and 1 ng (high) or 300 pg (low) of *fzd7* RNA for PKC-translocation assays in animal caps and 200 pg for *myc-dvl1*, *myc-dvl2*, *myc-dvl3*, *camkIIδ*, and *pkcα-GFP* in embryos for preparation of Keller explants. Knockdown of Dvl isoforms was achieved by injection of 1.6 pmol of the respective antisense MO oligonucleotides: Dvl2 MO, Dvl1 MO, and Dvl3 MO.

Embryos were injected at the two-cell stage for animal cap explants or at the four-cell stage in both dorsal blastomeres for Keller explants and cultured until they reached stage 10 or 10.5, respectively.

Keller open-face explants were prepared and cultured as described in Unterseher *et al.* (2004). Explants were scored as "normal elongation and constriction" if they showed >75% elongation and constriction, as "elongated with impaired constriction" if explants showed >75% elongation but failed to constrict, and "impaired elongation" if explants showed <75% elongation when compared with fully elongated control explants. Immunofluorescence staining of animal cap explants was performed as described previously (Tauriello *et al.*, 2012). Photographs were taken on a Zeiss Apotome imaging system (Zeiss, Oberkochen, Germany) and on a Leica SP5 confocal scanning microscope (Leica, Wetzlar, Germany).

Cell culture and transfection

HEK 293T human embryonic kidney cells (Leibniz Institute Collections of Microorganisms and Cell Culture, DSMZ, Braunschweig, Germany) were cultured in DMEM supplemented with 10% fetal calf serum (Life Technologies) at 37°C in a humidified atmosphere of 10% CO_2. Plasmid transfections were performed using Nanofectin (GE Healthcare, Freiburg, Germany) according to the manufacturer's protocols.

Coimmunopurifications and quantitative mass spectrometry

Plasmids encoding Arrb2-Flag, Dvl2-GFP, and hemagglutinin (HA)-tagged Gβ and Gγ were transiently transfected into HEK293T cells. Bait proteins were affinity isolated on anti-Flag beads (Sigma-Aldrich, Munich, Germany) or on anti-GFP beads prepared by coupling an anti-GFP antibody (Acris Antibodies, Herford, Germany) covalently to agarose beads (Direct IP Kit; Thermo Fisher Scientific, Bremen, Germany). Eluates were digested with trypsin and subsequently with Lys-C in solution. After addition of protein digests as quantitative standards, the samples were desalted on C-18 stage tips (Nest Group, Southborough, MA) and analyzed by nanoflow high-performance liquid chromatography–tandem mass spectrometry (2D-NanoLC; Eksigent, Dublin, CA; Orbitrap Velos MS, Thermo Fisher Scientific; Vasilj *et al.*, 2012). Protein identification was performed with Mascot V2.2 (Matrixscience, London, United Kingdom), and determination of peptide ion signals for label-free quantification was performed with Progenesis LCMS V2.6 (Nonlinear Dynamics, Newcastle on Tyne, United Kingdom); relative quantification was based on the most intense three signals (MI3; Silva *et al.*, 2006; Groessl *et al.*, 2012). Isoform specificity of peptides was obtained

from the proteomicsdb database (www.proteomicsdb.org; Wilhelm *et al.*, 2014).

Preparation of cell lysates, immunoprecipitation, and Western blotting

Cells were washed once with phosphate-buffered saline (PBS) and lysed in NP-40 buffer (20 mM Tris-HCl, pH 7.4, 150 mM NaCl, 2 mM EDTA, 1% NP-40) supplemented with Complete Protease Inhibitor and PhosStop Phosphatase Inhibitor Cocktails (Roche, Mannheim, Germany) at 4°C. For embryo lysates, embryos were collected at the desired stage and lysed in the same lysis buffer. Lysates were cleared at 16,000 × *g* for 10 min. For coimmunoprecipitation, lysates were incubated for 4 h at 4°C with the appropriate antibody and protein G–magnetic beads (Life Technologies) or anti-Flag M2 magnetic beads (Sigma-Aldrich). Immunoprecipitates were collected, washed four times with lysis buffer, and eluted with SDS sample buffer. For Western blotting, proteins were visualized colorimetrically with NBT/BCIP.

CamKII kinase activity assays

CamKII kinase activity assays were carried out according to the procedure described by Kühl *et al.* (2000a) with the following modifications: embryos were injected as indicated and cultured until stage 10.5. Embryos were lysed in 10 mM Tris-HCl, pH 7.5, 40 µM ethylene glycol tetraacetic acid, and 0.1% (vol/vol) β-mercaptoethanol supplemented with complete Protease Inhibitor and PhosStop Phosphatase Inhibitor cocktails (Roche, Mannheim, Germany) and cleared twice by centrifugation at 16,000 × *g* for 5 min. Protein concentrations were determined using a bicinchoninic acid assay (Applichem, Darmstadt, Germany) with bovine serum albumin as standard. The CamKII substrate Syntide-2 peptide PLARTLSVAGLPGKK (Hashimoto and Soderling, 1987) was custom synthesized and biotinylated at the N-terminus (PSL, Heidelberg, Germany). Per injection and batch, CamKII kinase activity was assayed as duplicates in 20-µl reactions (50 mM NH_4HCO_3/NH_4CH_3 COO, pH 7.5, 10 mM $MgCl_2$, 2 mM $CaCl_2$, 0.01 mM EDTA, 0.2 mM dithiothreitol, 100 µM ATP, 2.5 µM substrate peptide). Reactions were started by adding 2 µl cleared lysate, incubated for 2 min at 30°C, and stopped by adding 10 µl of 7.5 M guanidine HCl. The biotinylated substrate was captured on Streptavidin-coated magnetic beads (Life Technologies), washed twice with 2 M NaCl and twice with water and stored at –20°C until analysis. Immediately before analysis, beads were washed once more with water, the biotinylated peptide was released by incubation with 1 µl of 30% formic acid for ~1 min, and peptides were recovered for direct analysis with 20 µl of 45% acetonitrile and 2.85% formic acid in water. Samples were analyzed by static nano-electrospray with a Nanomate Triversa robotic ion source (Advion, Ithaca, NY) coupled to a Q-Exactive mass spectrometer (Thermo Fisher Scientific). Mass spectra were acquired at a nominal resolution of 140,000 at 200 *m/z* in centroid data mode. Thirty spectra were averaged, and the ratio of the intensities of the peptide ion signals of the phosphorylated and nonphosphorylated peptide was determined. Enzyme activities were calculated and are given in units (= picomoles/minute) per milligram of protein.

ACKNOWLEDGMENTS

We thank Michael Kühl, Gunnar Schulte, and Gary Davidson for generously providing plasmids, Annalen Bleckman for her help with statistics, and Hanh Nguyen for critical reading of the manuscript. We are grateful for helpful discussions with and support from Andrej Shevchenko. This work was funded by a research grant from the German Research Foundation (DFG) to A.S. (SCHA 965/6-1). M.G. was supported by the Max Planck Society (MPG).

REFERENCES

Bastock R, Strutt H, Strutt D (2003). Strabismus is asymmetrically localised and binds to Prickle and Dishevelled during Drosophila planar polarity patterning. Development 130, 3007–3014.

Behrens J, Jerchow BA, Würtele M, Grimm J, Asbrand C, Wirtz R, Kühl M, Wedlich D, Birchmeier W (1998). Functional interaction of an axin homolog, conductin, with beta-catenin, APC, and GSK3beta. Science 280, 596–599.

Bilic J, Huang Y-L, Davidson G, Zimmermann T, Cruciat C-M, Bienz M, Niehrs C (2007). Wnt induces LRP6 signalosomes and promotes dishevelled-dependent LRP6 phosphorylation. Science 316, 1619–1622.

Boutros M, Paricio N, Strutt DI, Mlodzik M (1998). Dishevelled activates JNK and discriminates between JNK pathways in planar polarity and wingless signaling. Cell 94, 109–118.

Brown SD, Twells RC, Hey PJ, Cox RD, Levy ER, Soderman AR, Metzker ML, Caskey CT, Todd JA, Hess JF (1998). Isolation and characterization of LRP6, a novel member of the low density lipoprotein receptor gene family. Biochem Biophys Res Commun 248, 879–888.

Bryja V, Gradl D, Schambony A, Arenas E, Schulte G (2007). Beta-arrestin is a necessary component of Wnt/beta-catenin signaling in vitro and in vivo. Proc Natl Acad Sci USA 104, 6690–6695.

Bryja V, Schambony A, Cajánek L, Dominguez I, Arenas E, Schulte G (2008). Beta-arrestin and casein kinase 1/2 define distinct branches of non-canonical WNT signalling pathways. EMBO Rep 9, 1244–1250.

Cadigan KM, Nusse R (1997). Wnt signaling: a common theme in animal development. Genes Dev 11, 3286–3305.

Choi S-C, Han J-K (2002). Xenopus Cdc42 regulates convergent extension movements during gastrulation through Wnt/Ca2 +signaling pathway. Dev Biol 244, 342–357.

Ciani L, Boyle KA, Dickins E, Sahores M, Anane D, Lopes DM, Gibb AJ, Salinas PC (2011). Wnt7a signaling promotes dendritic spine growth and synaptic strength through Ca^2 /Calmodulin-dependent protein kinase II. Proc Natl Acad Sci USA 108, 10732–10737.

Ciani L, Salinas PC (2007). c-Jun N-terminal kinase (JNK) cooperates with Gsk3beta to regulate Dishevelled-mediated microtubule stability. BMC Cell Biol 8, 27.

Clevers H (2006). Wnt/beta-catenin signaling in development and disease. Cell 127, 469–480.

Dabdoub A, Kelley MW (2005). Planar cell polarity and a potential role for a Wnt morphogen gradient in stereociliary bundle orientation in the mammalian inner ear. J Neurobiol 64, 446–457.

Darken RS, Scola AM, Rakeman AS, Das G, Mlodzik M, Wilson PA (2002). The planar polarity gene strabismus regulates convergent extension movements in Xenopus. EMBO J 21, 976–985.

Davidson G, Wu W, Shen J, Bilic J, Fenger U, Stannek P, Glinka A, Niehrs C (2005). Casein kinase 1 gamma couples Wnt receptor activation to cytoplasmic signal transduction. Nature 438, 867–872.

Dorsky RI, Moon RT, Raible DW (1998). Control of neural crest cell fate by the Wnt signalling pathway. Nature 396, 370–373.

Dunn KJ, Williams BO, Li Y, Pavan WJ (2000). Neural crest-directed gene transfer demonstrates Wnt1 role in melanocyte expansion and differentiation during mouse development. Proc Natl Acad Sci USA 97, 10050–10055.

Erondu NE, Kennedy MB (1985). Regional distribution of type II Ca2+/calmodulin-dependent protein kinase in rat brain. J Neurosci 5, 3270–3277.

Farr GH, Ferkey DM, Yost C, Pierce SB, Weaver C, Kimelman D (2000). Interaction among GSK-3, GBP, axin, APC in Xenopus axis specification. J Cell Biol 148, 691–702.

Funayama N, Fagotto F, McCrea P, Gumbiner BM (1995). Embryonic axis induction by the armadillo repeat domain of beta-catenin: evidence for intracellular signaling. J Cell Biol 128, 959–968.

Gao B, Song H, Bishop K, Elliot G, Garrett L, English MA, Andre P, Robinson J, Sood R, Minami Y, *et al.* (2011). Wnt signaling gradients establish planar cell polarity by inducing Vangl2 phosphorylation through Ror2. Dev Cell 20, 163–176.

Goto T, Keller R (2002). The planar cell polarity gene strabismus regulates convergence and extension and neural fold closure in Xenopus. Dev Biol 247, 165–181.

Gray RS, Bayly RD, Green SA, Agarwala S, Lowe CJ, Wallingford JB (2009). Diversification of the expression patterns and developmental functions of the dishevelled gene family during chordate evolution. Dev Dyn 238, 2044–2057.

Groessl M, Luksch H, Rösen-Wolff A, Shevchenko A, Gentzel M (2012). Profiling of the human monocytic cell secretome by quantitative label-free mass spectrometry identifies stimulus-specific cytokines and proinflammatory proteins. Proteomics 12, 2833–2842.

Habas R, Dawid IB, He X (2003). Coactivation of Rac and Rho by Wnt/Frizzled signaling is required for vertebrate gastrulation. Genes Dev 17, 295–309.
Habas R, Kato Y, He X (2001). Wnt/Frizzled activation of Rho regulates vertebrate gastrulation and requires a novel Formin homology protein Daam1. Cell 107, 843–854.
Hashimoto Y, Soderling TR (1987). Calcium · calmodulin-dependent protein kinase II and calcium. phospholipid-dependent protein kinase activities in rat tissues assayed with a synthetic peptide. Arch Biochem Biophys 252, 418–425.
Heisenberg CP, Tada M, Rauch GJ, Saúde L, Concha ML, Geisler R, Stemple DL, Smith JC, Wilson SW (2000). Silberblick/Wnt11 mediates convergent extension movements during zebrafish gastrulation. Nature 405, 76–81.
Ho H-YH, Susman MW, Bikoff JB, Ryu YK, Jonas AM, Hu L, Kuruvilla R, Greenberg ME (2012). Wnt5a-Ror-Dishevelled signaling constitutes a core developmental pathway that controls tissue morphogenesis. Proc Natl Acad Sci USA 109, 4044–4051.
Huelsken J, Vogel R, Erdmann B, Cotsarelis G, Birchmeier W (2001). beta-Catenin controls hair follicle morphogenesis and stem cell differentiation in the skin. Cell 105, 533–545.
Itoh K, Krupnik VE, Sokol SY (1998). Axis determination in Xenopus involves biochemical interactions of axin, glycogen synthase kinase 3 and beta-catenin. Curr Biol 8, 591–594.
Jenny A, Darken RS, Wilson PA, Mlodzik M (2003). Prickle and Strabismus form a functional complex to generate a correct axis during planar cell polarity signaling. EMBO J 22, 4409–4420.
Jenny A, Mlodzik M (2006). Planar cell polarity signaling: a common mechanism for cellular polarization. Mt Sinai J Med 73, 738–750.
Keller R (2005). Cell migration during gastrulation. Curr Opin Cell Biol 17, 533–541.
Kengaku M, Capdevila J, Rodriguez-Esteban C, La Peña, De J, Johnson RL, Izpisúa Belmonte JC, Tabin CJ (1998). Distinct WNT pathways regulating AER formation and dorsoventral polarity in the chick limb bud. Science 280, 1274–1277.
Kestler HA, Kühl M (2008). From individual Wnt pathways towards a Wnt signalling network. Philos Trans R Soc Lond B Biol Sci 363, 1333–1347.
Kiecker C, Niehrs C (2001). A morphogen gradient of Wnt/beta-catenin signalling regulates anteroposterior neural patterning in Xenopus. Development 128, 4189–4201.
Kim S-E, Huang H, Zhao M, Zhang X, Zhang A, Semonov MV, Macdonald BT, Zhang X, Garcia Abreu J, Peng L, *et al.* (2013). Wnt stabilization of β-catenin reveals principles for morphogen receptor-scaffold assemblies. Science 340, 867–870.
Kim G-H, Her J-H, Han J-K (2008). Ryk cooperates with Frizzled 7 to promote Wnt11-mediated endocytosis and is essential for Xenopus laevis convergent extension movements. J Cell Biol 182, 1073–1082.
Kispert A, Vainio S, McMahon AP (1998). Wnt-4 is a mesenchymal signal for epithelial transformation of metanephric mesenchyme in the developing kidney. Development 125, 4225–4234.
Kries von JP, Winbeck G, Asbrand C, Schwarz-Romond T, Sochnikova N, Dell'Oro A, Behrens J, Birchmeier W (2000). Hot spots in beta-catenin for interactions with LEF-1, conductin and APC. Nat Struct Biol 7, 800–807.
Krylova O, Messenger MJ, Salinas PC (2000). Dishevelled-1 regulates microtubule stability: a new function mediated by glycogen synthase kinase-3beta. J Cell Biol 151, 83–94.
Kühl M, Geis K, Sheldahl LC, Pukrop T, Moon RT, Wedlich D (2001). Antagonistic regulation of convergent extension movements in Xenopus by Wnt/beta-catenin and Wnt/Ca2 +signaling. Mech Dev 106, 61–76.
Kühl M, Sheldahl LC, Malbon CC, Moon RT (2000a). Ca(2+)/calmodulin-dependent protein kinase II is stimulated by Wnt and Frizzled homologs and promotes ventral cell fates in Xenopus. J Biol Chem 275, 12701–12711.
Kühl M, Sheldahl LC, Park M, Miller JR, Moon RT (2000b). The Wnt/Ca2+ pathway: a new vertebrate Wnt signaling pathway takes shape. Trends Genet 16, 279–283.
Lane MC, Keller R (1997). Microtubule disruption reveals that Spemann's organizer is subdivided into two domains by the vegetal alignment zone. Development 124, 895–906.
Li B, Mackay DR, Dai Q, Li TWH, Nair M, Fallahi M, Schonbaum CP, Fantes J, Mahowald AP, Waterman ML, *et al.* (2002). The LEF1/beta-catenin complex activates movo1, a mouse homolog of Drosophila ovo required for epidermal appendage differentiation. Proc Natl Acad Sci USA 99, 6064–6069.
Li L, Fothergill T, Hutchins BI, Dent EW, Kalil K (2014). Wnt5a evokes cortical axon outgrowth and repulsive guidance by tau mediated reorganization of dynamic microtubules. Dev Neurobiol 74, 797–817.
Logan CY, Nusse R (2004). The Wnt signaling pathway in development and disease. Annu Rev Cell Dev Biol 20, 781–810.
Lu X, Borchers AGM, Jolicoeur C, Rayburn H, Baker JC, Tessier-Lavigne M (2004). PTK7/CCK-4 is a novel regulator of planar cell polarity in vertebrates. Nature 430, 93–98.
Maloof JN, Whangbo J, Harris JM, Jongeward GD, Kenyon C (1999). A Wnt signaling pathway controls hox gene expression and neuroblast migration in C. elegans. Development 126, 37–49.
Marlow F, Topczewski J, Sepich D, Solnica-Krezel L (2002). Zebrafish Rho kinase 2 acts downstream of Wnt11 to mediate cell polarity and effective convergence and extension movements. Curr Biol 12, 876–884.
McKendry R, Hsu SC, Harland RM, Grosschedl R (1997). LEF-1/TCF proteins mediate wnt-inducible transcription from the Xenopus nodal-related 3 promoter. Dev Biol 192, 420–431.
Miller JR, Moon RT (1996). Signal transduction through beta-catenin and specification of cell fate during embryogenesis. Genes Dev 10, 2527–2539.
Minami Y, Oishi I, Endo M, Nishita M (2010). Ror-family receptor tyrosine kinases in noncanonical Wnt signaling: their implications in developmental morphogenesis and human diseases. Dev Dyn 239, 1–15.
Moon RT, Campbell RM, Christian JL, McGrew LL, Shih J, Fraser S (1993). Xwnt-5A: a maternal Wnt that affects morphogenetic movements after overexpression in embryos of Xenopus laevis. Development 119, 97–111.
Nakamura T, Sano M, Songyang Z, Schneider MD (2003). A Wnt- and beta -catenin-dependent pathway for mammalian cardiac myogenesis. Proc Natl Acad Sci USA 100, 5834–5839.
Nieuwkoop PD, Faber J (1975). External and internal stage criteria in the development of Xenopus laevis. Normal Tables of Xenopus laevis, Amsterdam: North-Holland, 162–188.
Nishita M, Itsukushima S, Nomachi A, Endo M, Wang Z, Inaba D, Qiao S, Takada S, Kikuchi A, Minami Y (2010). Ror2/Frizzled complex mediates Wnt5a-induced AP-1 activation by regulating dishevelled polymerization. Mol Cell Biol 30, 3610–3619.
Oishi I, Suzuki H, Onishi N, Takada R, Kani S, Ohkawara B, Koshida I, Suzuki K, Yamada G, Schwabe GC, *et al.* (2003). The receptor tyrosine kinase Ror2 is involved in non-canonical Wnt5a/JNK signalling pathway. Genes Cells 8, 645–654.
Penzo-Mendèz A, Umbhauer M, Djiane A, Boucaut J-C, Riou J-F (2003). Activation of Gbetagamma signaling downstream of Wnt-11/Xfz7 regulates Cdc42 activity during Xenopus gastrulation. Dev Biol 257, 302–314.
Peters JM, McKay RM, McKay JP, Graff JM (1999). Casein kinase I transduces Wnt signals. Nature 401, 345–350.
Rosso SB, Sussman D, Wynshaw-Boris A, Salinas PC (2005). Wnt signaling through Dishevelled, Rac and JNK regulates dendritic development. Nat Neurosci 8, 34–42.
Sakanaka C, Leong P, Xu L, Harrison SD, Williams LT (1999). Casein kinase iepsilon in the wnt pathway: regulation of beta-catenin function. Proc Natl Acad Sci USA 96, 12548–12552.
Saneyoshi T, Kume S, Amasaki Y, Mikoshiba K (2002). The Wnt/calcium pathway activates NF-AT and promotes ventral cell fate in Xenopus embryos. Nature 417, 295–299.
Schambony A, Wedlich D (2007). Wnt-5A/Ror2 regulate expression of XPAPC through an alternative noncanonical signaling pathway. Dev Cell 12, 779–792.
Schneider S, Steinbeisser H, Warga RM, Hausen P (1996). Beta-catenin translocation into nuclei demarcates the dorsalizing centers in frog and fish embryos. Mech Dev 57, 191–198.
Seïtz K, Dürsch V, Harnoš J, Bryja V, Gentzel M, Schambony A (2014). β-arrestin interacts with the beta/gamma subunits of trimeric G-proteins and Dishevelled in the Wnt/Ca2+ pathway in Xenopus gastrulation. PLoS One 9, e87132.
Semenov MV, Habas R, Macdonald BT, He X (2007). SnapShot: noncanonical Wnt signaling pathways. Cell 131, 1378.
Sheldahl LC, Park M, Malbon CC, Moon RT (1999). Protein kinase C is differentially stimulated by Wnt and Frizzled homologs in a G-protein-dependent manner. Curr Biol 9, 695–698.
Sheldahl LC, Slusarski DC, Pandur P, Miller JR, Kühl M, Moon RT (2003). Dishevelled activates Ca2+ flux, PKC, and CamKII in vertebrate embryos. J Cell Biol 161, 769–777.
Silva JC, Gorenstein MV, Li G-Z, Vissers JPC, Geromanos SJ (2006). Absolute quantification of proteins by LCMSE: a virtue of parallel MS acquisition. Mol Cell Proteomics 5, 144–156.

Simões S de M, Blankenship JT, Weitz O, Farrell DL, Tamada M, Fernandez-Gonzalez R, Zallen JA (2010). Rho-kinase directs Bazooka/Par-3 planar polarity during Drosophila axis elongation. Dev Cell 19, 377–388.
Slusarski DC, Corces VG, Moon RT (1997a). Interaction of Wnt and a Frizzled homologue triggers G-protein-linked phosphatidylinositol signalling. Nature 390, 410–413.
Slusarski DC, Yang-Snyder J, Busa WB, Moon RT (1997b). Modulation of embryonic intracellular Ca2+ signaling by Wnt-5A. Dev Biol 182, 114–120.
Strutt DI, Weber U, Mlodzik M (1997). The role of RhoA in tissue polarity and Frizzled signalling. Nature 387, 292–295.
Tada M, Smith JC (2000). Xwnt11 is a target of Xenopus Brachyury: regulation of gastrulation movements via Dishevelled, but not through the canonical Wnt pathway. Development 127, 2227–2238.
Tadjuidje E, Cha S-W, Louza M, Wylie C, Heasman J (2011). The functions of maternal Dishevelled 2 and 3 in the Early Xenopus embryo. Dev Dyn 240, 1727–1736.
Tamai K, Semenov M, Kato Y, Spokony R, Liu C, Katsuyama Y, Hess F, Saint-Jeannet JP, He X (2000). LDL-receptor-related proteins in Wnt signal transduction. Nature 407, 530–535.
Tauriello DVF, Jordens I, Kirchner K, Slootstra JW, Kruitwagen T, Bouwman BAM, Noutsou M, Rüdiger SGD, Schwamborn K, Schambony A, *et al.* (2012). Wnt/β-catenin signaling requires interaction of the Dishevelled DEP domain and C terminus with a discontinuous motif in Frizzled. Proc Natl Acad Sci USA 109, E812–E820.
Tetsu O, McCormick F (1999). Beta-catenin regulates expression of cyclin D1 in colon carcinoma cells. Nature 398, 422–426.
Tobimatsu T, Fujisawa H (1989). Tissue-specific expression of four types of rat calmodulin-dependent protein kinase II mRNAs. J Biol Chem 264, 17907–17912.
Unterseher F, Hefele JA, Giehl K, De Robertis EM, Wedlich D, Schambony A (2004). Paraxial protocadherin coordinates cell polarity during convergent extension via Rho A and JNK. EMBO J 23, 3259–3269.
van Amerongen R (2012). Alternative Wnt pathways and receptors. Cold Spring Harb Perspect Biol 4, a007914–a007914.
Vasilj A, Gentzel M, Ueberham E, Gebhardt R, Shevchenko A (2012). Tissue proteomics by one-dimensional gel electrophoresis combined with label-free protein quantification. J Proteome Res 11, 3680–3689.
Verkaar F, Zaman GJR (2010). A model for signaling specificity of Wnt/Frizzled combinations through co-receptor recruitment. FEBS Lett 584, 3850–3854.
Wallingford JB, Goto T, Keller R, Harland RM (2002). Cloning and expression of Xenopus Prickle, an orthologue of a Drosophila planar cell polarity gene. Mech Dev 116, 183–186.
Wallingford JB, Rowning BA, Vogeli KM, Rothbächer U, Fraser SE, Harland RM (2000). Dishevelled controls cell polarity during Xenopus gastrulation. Nature 405, 81–85.
Wallingford JB, Vogeli KM, Harland RM (2001). Regulation of convergent extension in Xenopus by Wnt5a and Frizzled-8 is independent of the canonical Wnt pathway. Int J Dev Biol 45, 225–227.
Wang J, Hamblet NS, Mark S, Dickinson ME, Brinkman BC, Segil N, Fraser SE, Chen P, Wallingford JB, Wynshaw-Boris A (2006). Dishevelled genes mediate a conserved mammalian PCP pathway to regulate convergent extension during neurulation. Development 133, 1767–1778.
Wang Q, Symes AJ, Kane CA, Freeman A, Nariculam J, Munson P, Thrasivoulou C, Masters JRW, Ahmed A (2010). A novel role for Wnt/Ca2+signaling in actin cytoskeleton remodeling and cell motility in prostate cancer. PLoS One 5, e10456.
Wilhelm M, Schlegl J, Hahne H, Moghaddas Gholami A, Lieberenz M, Savitski MM, Ziegler E, Butzmann L, Gessulat S, Marx H, *et al.* (2014). Mass-spectrometry-based draft of the human proteome. Nature 509, 582–587.
Willert K, Brink M, Wodarz A, Varmus H, Nusse R (1997). Casein kinase 2 associates with and phosphorylates dishevelled. EMBO J 16, 3089–3096.
Winklbauer R, Medina A, Swain RK, Steinbeisser H (2001). Frizzled-7 signalling controls tissue separation during Xenopus gastrulation. Nature 413, 856–860.
Wu J, Mlodzik M (2009). A quest for the mechanism regulating global planar cell polarity of tissues. Trends Cell Biol 19, 295–305.
Yamanaka H, Moriguchi T, Masuyama N, Kusakabe M, Hanafusa H, Takada R, Takada S, Nishida E (2002). JNK functions in the non-canonical Wnt pathway to regulate convergent extension movements in vertebrates. EMBO Rep 3, 69–75.